Identification of Motile Sperm Domain Containing 1 (MOSPD1) As a Novel Target of the Wnt/β-Catenin Signaling Pathway in Colorectal Cancer

Chiaki Horie
The University of Tokyo
Chi Zhu
The University of Tokyo
Kiyoshi Yamaguchi (kiyamagu@g.ecc.u-tokyo.ac.jp)
The University of Tokyo
Saya Nakagawa
The University of Tokyo
Kiyoko Takane
The University of Tokyo
Tsuneo Ikenoue
The University of Tokyo
Yasunori Ohta
The University of Tokyo
Yukihisa Tanaka
The University of Tokyo
Susumu Aikou
The University of Tokyo
Giichiro Tsurita
The University of Tokyo
Yuka Ahiko
The University of Tokyo
Dai Shida
The University of Tokyo
Yoichi Furukawa
The University of Tokyo

Research Article

Keywords: crucial role, MOSPD1, ChIP-qPCR, TCF-binding

Posted Date: September 22nd, 2021

DOI: https://doi.org/10.21203/rs.3.rs-910485/v1

Identification of motile sperm domain containing 1 (*MOSPD1*) as a novel target of the Wnt/β-catenin signaling pathway in colorectal cancer

Chiaki Horie[1#], Chi Zhu[1#], Kiyoshi Yamaguchi[1*], Saya Nakagawa[1], Kiyoko Takane[1], Tsuneo Ikenoue[1], Yasunori Ohta[2], Yukihisa Tanaka[2], Susumu Aikou[3], Giichiro Tsurita[3], Yuka Ahiko[3], Dai Shida[3], Yoichi Furukawa[1]

[1]Division of Clinical Genome Research, Institute of Medical Science, The University of Tokyo, Tokyo 108-8639, Japan
[2]Department of Pathology, Research Hospital, Institute of Medical Science, The University of Tokyo, Tokyo 108-8639, Japan
[3]Department of Surgery, Research Hospital, Institute of Medical Science, The University of Tokyo, Tokyo 108-8639, Japan

[#]These authors contributed equally to this work.

[*]To whom correspondence should be addressed:
Kiyoshi Yamaguchi, Ph.D.
Division of Clinical Genome Research, Advanced Clinical Research Center
Institute of Medical Science, The University of Tokyo
4-6-1 Shirokanedai, Minato-ku, Tokyo 108-8639, Japan
Phone: +81-3-6409-2106
Fax: +81-3-6409-2103
E-mail: kiyamagu@g.ecc.u-tokyo.ac.jp

Abstract

Aberrant activation of the Wnt/β-catenin signaling pathway plays a crucial role in the development and progression of colorectal cancer. Previously, we identified a set of candidate genes that were regulated by this signaling pathway, and we focused on *MOSPD1*, motile sperm domain containing 1, in this study. Immunohistochemical staining revealed that the expression of MOSPD1 was elevated in tumorous cells of colorectal cancer tissues compared with non-tumorous cells. Using ChIP-seq data and JASPAR database, we searched for the regulatory region(s) in the *MOSPD1* gene as a target of the Wnt/β-catenin signaling, and identified a region containing three putative TCF-binding motifs in the 3'-flanking region. Additional analyses using reporter assay and ChIP-qPCR suggested that this region harbors an enhancer activity through an interaction with TCF7L2 and β-catenin. These data have clarified that *MOSPD1* is a novel direct target of the Wnt/β-catenin signaling. In addition, the identification of its enhancer region may be helpful for the future studies of precise regulatory mechanisms of MOSPD1.

Introduction

The Wnt/β-catenin signaling pathway (also known as the canonical Wnt pathway) is responsible for embryonic development and tissue homeostasis[1]. Aberrant activation of this pathway by genetic and epigenetic alteration is involved in human diseases such as cancer[2,3,4]. In colorectal cancer (CRC), frequent activation of Wnt/β-catenin signaling pathway by somatic mutations in APC regulator of WNT signaling pathway (*APC*) or the β-catenin gene (*CTNNB1*) has been reported. In the cBioPortal for Cancer Genomics (https://www.cbioportal.org/), a public database of cancer genomes, mutations of *APC* and *CTNNB1* were found in 64% and 6%, respectively, of 3,051 CRC tissues. Loss of function mutations in *APC* or activating mutations in *CTNNB1* results in the stabilization and accumulation of β-catenin protein in the cells. The accumulated β-catenin interacts with T cell factor (TCF) / lymphoid enhancer-binding factor (LEF) transcription factors in the nucleus, and induces the expression of their target genes (Wnt target genes)[5]. To date, more than one hundred Wnt target genes have been identified, and a list of the genes is shown on the Wnt homepage at https://web.stanford.edu/group/nusselab/cgi-bin/wnt/target_genes. Studies of their function have helped to further understand

the molecular mechanisms of carcinogenesis, and the complex regulatory mechanisms underlying this signaling pathway. Representative examples of the aberrant activation of this pathway contributing to carcinogenesis include MYC proto-oncogene (*MYC*) and cyclin D1 (*CCND1*). *MYC* was identified by serial analysis of gene expression using HT29 cells containing a zinc-inducible APC, and affects a wide variety of functions such as cell proliferation, angiogenesis, and promotion of anaerobic metabolism[6]. *Cyclin D1* is known to regulate G1-S cell cycle progression, and it was identified through the analysis of human genes involved in controlling cell growth, the promoter regions of which contain the core TCF/LEF-binding sites[7].

It is of note that chromatin immunoprecipitation coupled with high-throughput sequencing (ChIP-seq) analysis using six different cell lines and anti-TCF7L2 antibody identified 116,000 non-redundant TCF7L2-binding sites, with 1,864 sites common to the cell lines tested, suggesting the existence of as yet unidentified Wnt target genes in human cells[8]. To understand the precise molecular mechanism underlying the development of Wnt-driven cancer, we previously searched for new target genes by microarray using β-catenin-depleted CRC cells and ChIP-seq of TCF7L2. Integrated analysis of these data identified

11 candidate genes that are directly regulated by the β-catenin/TCF7L2 complex[9]. Among these candidates, we focused in this study on motile sperm domain containing 1 (*MOSPD1*), and revealed that *MOSPD1* is a novel direct target of the Wnt signaling pathway. Furthermore, we identified three Wnt responsive elements in the 3'-flanking region of *MOSPD1*, and showed that the elements are involved in the transcriptional activation. These data will help deepen our understanding of colorectal carcinogenesis, as well as the regulatory mechanism of MOSPD1.

Results

The expression of MOSPD1 is regulated by Wnt/β-catenin signaling in colorectal cancer cells

In the previous study, we identified a total of 11 target genes whose expression was commonly down-regulated by the introduction of β-catenin siRNAs and a dominant-negative form of TCF7L2 (dnTCF7L2) in HCT116, SW480, and LS174T cells[9]. Subsequent qPCR analysis revealed that the expression of *PDE4D*, *PHLDB2*, *OXR1*, *FRMD5*, and *MOSPD1* was significantly decreased by the

knockdown of β-catenin. To verify the association of MOSPD1 with the Wnt/β-catenin signaling, we performed western blot analysis using lysates from SW480 and HCT116 cells treated with β-catenin or control siRNA. In agreement with the qPCR data, treatment with two independent β-catenin siRNAs decreased MOSPD1 expression in both cells (Fig. 1a). In addition, treatment of HeLa cells with lithium chloride (LiCl), a glycogen synthase kinase 3 (GSK3) inhibitor that activates the Wnt/β-catenin signaling, increased β-catenin and MOSPD1 expression (Fig. 1b). These data corroborated that MOSPD1 is a downstream target of the Wnt/β-catenin signaling.

Since aberrant activation of the Wnt/β-catenin signaling is involved in the majority of CRC[2,10], we searched for gene expression data of colorectal tumors in NCBI Gene Expression Omnibus. In a dataset (GSE21510) containing 104 CRC tissues and 25 non-tumorous colonic tissues[11], the average *MOSPD1* expression was found to be 2.18-fold higher (q-value: $3.05E^{-13}$) in the tumor tissues than in the non-tumorous tissues (Fig. 1c). In addition, the expression levels showed a positive correlation with *RNF43* (r^2=0.40), *AXIN2* (r^2=0.30), and *MYC* (r^2=0.29), three well-known Wnt targets (Fig. 1d). These data supported that *MOSPD1* expression is induced by the activation of Wnt signaling.

We further carried out immunohistochemical staining of β-catenin and MOSPD1 using 11 CRC tissues. As shown in Fig. 1e, β-catenin was stained in the cytoplasm and/or nucleus of tumorous cells in all tumor tissues tested (upper panel). In addition, MOSPD1 was also positively stained in the cytoplasm and/or nucleus of the tumorous cells (Fig. 1e, lower panel).

Identification of an enhancer in the 3'-flanking region of *MOSPD1*

In our previous study, ChIP-seq analysis showed a region for the binding with TCF7L2 in the 3'-flaking region of *MOSPD1* (3'-putative enhancer, GRCh38-chrX:134,885,306-134,886,672)[9]. This region was overlapped with a peak in ENCODE ChIP-seq data of TCF7L2 (ENCSR000EUV, Fig. 2a, upper panel). In addition to the 3'-region, the ENCODE data showed another peak in the 5'-flanking region of *MOSPD1* (GRCh38-chrX: 134,932,561-134,932,930). These peaks were overlapped with peaks of histone modifications (H3K4me1: ENCSR161MXP and H3K27Ac: ENCSR000EUT, Fig. 2a, middle and lower panels), suggesting that these regions may have enhancer activity through the interaction with TCF7L2. To investigate their enhancer activity, these regions were cloned into reporter plasmids, and reporter assays were performed using

HCT116 cells. As a result, both reporter plasmids, pGL4.23-MOSPD1-5'E and pGL4.23-MOSPD1-3'E, showed increased reporter activity compared to the mock reporter (empty) by 1.29- and 5.62-fold, respectively (Fig. 2b). Importantly, co-transfection of the reporter plasmids with plasmids expressing a dominant-negative form of TCF7L2 (dnTCF7L2) significantly decreased the reporter activity of pGL4.23-MOSPD1-3'E, but not the activity of pGL4.23-MOSPD1-5'E, suggesting the enhancer activity of the 3'-flanking region through the interaction with TCF7L2. In addition, knockdown of β-catenin by two independent siRNAs markedly reduced the reporter activity of pGL4.23-MOSPD1-3'E (Fig. 2c).

To confirm the interaction between the 3'-flanking region of *MOSPD1* and TCF7L2, we performed an additional ChIP-qPCR assay using anti-TCF7L2 antibody and region-specific primer sets for the 3'-enhancer region of *MOSPD1.* An enhancer region in intron 2 of *RNF43* was recruited as a positive control[12]. This assay detected an enrichment of the enhancer region in *RNF43* by 4.53-fold in the precipitants with the anti-TCF7L2 antibody compared to those with normal IgG. DNA fragments containing the 3'-enhancer region of *MOSPD1* were enriched by 10.3-fold in the precipitants (Fig. 2d). These data suggested that both TCF7L2 and β-catenin are involved in the enhancer activity and that TCF7L2

associates with the 3'-enhancer region.

Involvement of three TCF-binding motifs in the enhancer activity

We further searched for TCF-binding elements (TBE) in the 3'-enhancer region using JASPAR, a database for transcription factor binding profiles[13], and identified eight candidate TBEs (Supplementary Table S1). Among the eight, we focused on three TBEs with a similarity score greater than 10; TBE1 (GRCh38-chrX: 134,885,716-134,885,729), TBE2 (GRCh38-chrX: 134,885,543-134,885,556), and TBE3 (GRCh38-chrX: 134,885,482-134,885,495). To investigate the involvement of these motifs in the enhancer activity, we prepared mutant reporter plasmids containing two-nucleotide substitutions in each TCF-binding motif (TBE1-mut, TBE2-mut, and TBE3-mut) of pGL4.23-MOSPD1-3'E and reporter plasmids containing these substitutions in the three motifs (TBEall-mut) (Fig. 3a). A reporter assay determined that the reporter activity of mutant plasmids (TBE1-mut, TBE2-mut, and TBE3-mut) was significantly reduced compared to the wild type plasmids (pGL4.23-MOSPD1-3'E) by 9.87%, 35.3%, and 35.0%, respectively. In addition, the activity of TBEall-mut plasmids was markedly decreased compared to the wild type by 85.6% (Fig. 3b). Treatment of

the cells expressing TBE1-mut, TBE2-mut, or TBE3-mut with β-catenin siRNA suppressed the activity by 50.2%, 52.2%, and 42.3%, respectively, compared to the cells with control siRNA. These data indicated that the three motifs are, at least in part, associated with the enhancer activity of TCF7L2.

Discussion

In this study, we revealed for the first time that *MOSPD1* is transcriptionally regulated by Wnt signaling through the three TBEs located in its 3'-flanking region.

MOSPD1 is a member of major sperm protein (MSP) domain-containing family that is highly conserved in many species. There are three MSP domain-containing proteins (MOSPD1, 2, and 3) in humans, and four (Mospd1, 2, 3, and 4) in mice and rats[14]. The similarities between human MOSPD1 and human MOSPD2, and that between human MOSPD1 and human MOSPD3 are 8% and 32%, respectively, at protein levels (CLUSTALW, https://www.genome.jp/tools-bin/clustalw). In our previous expression profile analysis, knockdown of β-catenin decreased *MOSPD1* expression by 38% in SW480 cells, but it increased the expression of *MOSPD2* and *MOSPD3* by 20% and 40%, respectively. These data

may imply that MOSPD1 has a specific function that is linked with the canonical Wnt signaling pathway in development.

The function of MOSPD1 is still largely unclarified. In the early 1980s, MSP was isolated as a protein 15K from sperm cells of *Caenorhabditis elegans*[15], implying its role in spermatogenesis. Later, MSP was shown to function as a motility apparatus in sperm locomotion[16,17]. In GTEx Portal, a public database of gene expression in normal tissues (https://gtexportal.org/home/), *MOSPD1* is expressed in a variety of tissues including esophageal mucosa, adrenal gland, testis, skin, and uterus, suggesting that MOSPD1 should play physiological role(s) in various tissues. In mice, *Mospd1* is abundantly expressed in mesenchymal tissues, and its expression is elevated during differentiation in osteoblastic, myoblastic, and adipocytic cell lines[14]. Another study revealed that Mospd1-null embryonic stem cells were able to proliferate and that they were unable to differentiate to osteoblasts, adipocytes, and hematopoietic progenitors[18]. These data indicated that Mospd1 should be involved in the differentiation and proliferation of mesenchymal cells. In addition, knockdown of *Mospd1* induced the expression of epithelial cadherin *Cdh1*, and decreased the expression of *Snail1*, *Snai2*, and mesenchymal cadherin *Cdh11* in MC3T3-E1

cells established from mouse osteoblasts[14]. These results suggested that Mospd1 may be associated with epithelial-mesenchymal transition (EMT). Interestingly, expression of *Runx2* and *Osteocalcin* was also down-regulated by the knockdown of *Mospd1* in MC3T3-E1 cells[14]. RUNX2, one of the transcription factors required for osteoblastic differentiation is abundantly expressed in the nucleus of osteoid osteoma cells[19]. In addition, a study reported that surgical resection of osteoid osteoma in two patients decreased total and undercarboxylated osteocalcin in their sera, suggesting that osteocalcin is secreted by the osteoid osteoma cells[20]. It is noteworthy that osteomas frequently develop in the mandible bone of patients with germline variants in the *APC* gene[21]. The induction of RUNX2 and/or osteocalcin by the increased expression of MOSPD1 in osteoblasts may be involved in the development of osteomas in FAP patients.

We have shown here that the expression of MOSPD1 is elevated in all CRC tissues examined, and that its expression is associated with the accumulation of β-catenin. The expression of MOSPD1 was shown to be elevated in the circulating tumor cells of metastatic castration-resistant prostate cancer[22]. It was also reported that abnormal β-catenin expression was observed

in approximately 38% of hormone-refractory prostate cancer, which is much higher than that detected in prostate cancer tissues obtained from radical prostatectomy[23]. Since MOSPD1 expression is associated with EMT, up-regulation of MOSPD1 in cancer cells may be related to their invasion and metastasis. In line with this view, ovarian cancer cells with high invasion-phenotype expressed significantly increased levels of MOSPD1 compared to the cells with low invasion-phenotype[24]. Although further studies are necessary, augmented expression of MOSPD1 may play a crucial role in the EMT of CRC.

We identified a distant enhancer region for the Wnt/β-catenin signaling in the 3'-flanking region *of MOSPD1*. Enhancer regions that associate with β-catenin-TCF/LEF1 complexes have been identified in various regions of the target genes. For instance, the enhancer regions of *MYC*[6], *CCND1*[7], claudin-1 (*CLDN1*)[25], membrane-type matrix metalloproteinase (*MT1-MMP*)[26], and *SP5*[27] are localized in their 5'-flanking regions, and those of *RNF43*[12] and *FRMD5*[9] in intron 2 and intron 1, respectively. Regarding *AXIN2*, several enhancer regions have been discovered in its 5'-flanking region and in intron 1[28]. It is of note that, in addition to the 5'-flanking enhancer region, *MYC* has another enhancer element in its 3'-flanking region[29]. Therefore, *MOSPD1* may have additional

enhancer region(s) in addition to the one identified here.

In conclusion, we have discovered that *MOSPD1* is a novel target gene of the Wnt signaling pathway in CRC. Further analysis of MOSPD1 function will elucidate the precise molecular mechanism underlying the development and progression of CRC, and may contribute to the development of therapeutic strategies against their invasion and metastasis.

Materials and methods

Cell culture

Human CRC cell lines, HCT116 and SW480, and a human cervix cell line, HeLa were purchased from the American Type Culture Collection (Manassas, VA). All cell lines were grown in appropriate media (McCoy's 5a Modified Medium for HCT116, Leibovitz's L-15 Medium for SW480, and Eagle’s Minimum Essential Medium for HeLa) supplemented with 10% fetal bovine serum (BioSera, Boussens, France), and antibiotic/antimycotic solution (Fujifilm Wako Pure Chemical, Osaka, Japan). HCT116 and HeLa cells were maintained in 5% CO_2 at 37°C, and SW480 cells were maintained without CO_2 supplementation at 37°C.

Reporter plasmids and luciferase assay

Two genomic regions of 5'-putative (GRCh38-chrX: 134,932,384-134,933,013) and 3'-putative enhancers (GRCh38-chrX: 134,885,255-134,886,704) were amplified by PCR using region-specific primer sets and genomic DNA extracted from the peripheral blood of healthy volunteers as a template. After digestion with *Xho*I and *Bgl*II restriction enzymes, the PCR products were cloned into pGL4.23 vector (Promega, Madison, WI) to generate pGL4.23-MOSPD1-5'E and pGL4.23-MOSPD1-3'E. The primer sequences are shown in Supplementary Table S2. HCT116 cells were transfected with these reporter plasmids together with control or β-catenin siRNAs using Lipofectamine 2000 (Thermo Fisher Scientific, Waltham, MA). pRL-null plasmids were co-transfected with the reporter plasmids for normalization. 48 hours after the transfection, the cells were lysed and reporter activities were measured using dual luciferase kit (TOYO B-Net, Tokyo, Japan) and Lumat LB9507 Luminometer (Berthold Technologies, Bad Wildbad, Germany). Firefly luciferase activities were normalized to *Renilla* luciferase activity (pRL-null).

Site-directed mutagenesis

Mutant reporter plasmids containing substitutions in the consensus sequence of the TCF7L2-binding motifs were prepared by site-directed mutagenesis. Wild type-plasmid DNA of pGL4.23-MOSPD1-3'E was amplified using KOD-Plus-Neo (Toyobo, Osaka, Japan) and a set of mutagenic primers (Supplementary Table S3). The PCR products were digested with *Dpn*I restriction enzyme (Takara Bio, Shiga, Japan) to cleave the methylated template DNA, followed by transformation into *Escherichia coli*. Insertion of mutations in the plasmids was confirmed by Sanger sequencing (3500xl DNA Analyzer, Thermo Fisher Scientific).

Gene silencing

For the knockdown of β-catenin, two β-catenin siRNAs (siβ-catenin#9: 5'-GAUCCUAGCUAUCGUUCUU-3' and siβ-catenin#10: 5'-UAAUGAGGACCUAUACUUA-3', Merck, Darmstadt, Germany) were used. Control siRNA (siControl, ON-TARGET plus Non-targeting Pool, #D-001810-10-20) was purchased from Horizon Discovery (Lafayette, CO). Cells were transfected with 10 nM of the indicated siRNA using Lipofectamine RNAiMAX or Lipofectamine 2000 (Thermo Fisher Scientific) for 48 hours.

Western blotting

Total protein was extracted from cultured cells using SDS sample buffer (25 mM Tris-HCl, pH6.8, 0.8% sodium dodecyl sulfate, 4% glycerol). After boiling the samples for 10 min, the protein was separated by SDS-PAGE, and transferred onto a nitrocellulose membrane (GE Healthcare, Buckinghamshire, UK). The membranes were blocked with 5% milk in TBS-T (Tris-buffered saline - Tween20), and then incubated with primary antibody; anti-MOSPD1 (GTX32111, GeneTex, Irvine, CA), anti-β-catenin (9582, Cell Signaling Technology, Danvers, MA), or anti-β-actin antibodies (A5441, Merck). Horseradish peroxidase-conjugated goat anti-mouse or anti-rabbit IgG (GE Healthcare) served as the secondary antibody for the ECL Detection System (GE Healthcare).

Chromatin immunoprecipitation assay

Chromatin immunoprecipitation followed by qPCR (ChIP-qPCR) was performed as described previously[30]. Briefly, HCT116 cells were cross-linked with 1% formaldehyde for 10 min at room temperature, and 0.1 M glycine was added to quench the formaldehyde. Chromatin was extracted and sheared by micrococcal

nuclease digestion (New England Biolabs, Ipswich, MA). Subsequently, protein-DNA complexes were immunoprecipitated with 10 µg of anti-TCF7L2 antibody (05−511, Merck) bound to Dynabeads Protein G (Thermo Fisher Scientific). Normal mouse IgG (Santa Cruz Biotechnology, Santa Cruz, CA) was used as a negative control. The precipitated protein-DNA complexes were purified by conventional DNA extraction methods, and the purified DNA was subjected to qPCR analysis using KAPA SYBR FAST ABI prism Kit (Kapa Biosystems, Wilmington, MA) and a set of primers encompassing the TCF-binding motifs located in the 3'-flanking region of *MOSPD1*. Amplification of a region upstream of the *GAPDH* gene was used as a negative control. Sequences of the primers are shown in Supplementary Table S4.

Immunohistochemical staining

Tissue sections were deparaffinized with xylene and rehydrated in a graded series of ethanol. Antigen retrieval was performed using 0.01 M citrate buffer (pH6.0) and autoclave heating at 110°C for 10 min. After blocking endogenous peroxidase activity in 0.3% H_2O_2 (Fujifilm Wako Pure Chemical) for 5 min, slides were incubated with 5% goat serum (ab7481, Abcam, Cambridge, UK) for 8 min,

followed by the incubation with anti-MOSPD1 (GeneTex, 1:200) or anti-β-catenin antibody (RB-1491, NeoMarkers, Union City, CA, 1:300) at 4°C overnight. Secondary antibody, Dako EnVisionTM+ Dual Link System-HRP (Dako, Carpentaria, CA), and ImmPACT DAB Substrate Kit (Vecter laboratories, Burlingame, CA) were then used to visualize the immunoreactivity. Tissue sections were counterstained with hematoxylin (Merck).

This study was approved by the ethical committee of the Institute of Medical Science, The University of Tokyo (IMSUT-IRB, 2020-78-0318). All colorectal tumor tissues and corresponding non-cancerous tissues were obtained with informed consent from the resected specimens of patients who underwent surgery or endoscopy. All methods were carried out in accordance with relevant guidelines and regulations.

Data Availability

All data generated or analyzed during this study are included in this published article.

Reference

1. Clevers, H. Wnt/β-catenin signaling in development and disease. *Cell* **127**, 469–480 (2006).
2. Voloshanenko, O. *et al.* Wnt secretion is required to maintain high levels of Wnt activity in colon cancer cells. *Nat. Commun.* **4**, 2610 (2013).
3. Wang, W. *et al.* Blocking Wnt secretion reduces growth of hepatocellular carcinoma cell lines mostly independent of β-catenin signaling. *Neoplasia* **18**, 711–723 (2016).
4. Cleary, A. S., Leonard, T. L., Gestl, S. A. & Gunther, E. J. Tumour cell heterogeneity maintained by cooperating subclones in Wnt-driven mammary cancers. *Nature* **508**, 113–117 (2014).
5. Behrens, J. *et al.* Functional interaction of β-catenin with the transcription factor LEF-1. *Nature* **382**, 638–642 (1996).
6. He, T. C. *et al.* Identification of c-MYC as a target of the APC pathway. *Science* **281**, 1509–12 (1998).
7. Tetsu, O. & McCormick, F. β-catenin regulates expression of cyclin D1 in colon carcinoma cells. *Nature* **398**, 422–426 (1999).
8. Frietze, S. *et al.* Cell type-specific binding patterns reveal that TCF7L2 can be tethered to the genome by association with GATA3. *Genome Biol.* **13**, R52 (2012).
9. Zhu, C. *et al.* Identification of FERM domain-containing protein 5 as a novel target of β-catenin/TCF7L2 complex. *Cancer Sci.* **108**, 612–619 (2017).
10. Schatoff, E. M., Leach, B. I. & Dow, L. E. Wnt signaling and colorectal cancer. *Current Colorectal Cancer Reports* **13**, 101–110 (2017).
11. Tsukamoto, S. *et al.* Clinical significance of osteoprotegerin expression in human colorectal cancer. *Diagnosis* (2011). doi:10.1158/1078-0432.CCR-10-2884
12. Takahashi, N., Yamaguchi, K., Ikenoue, T., Fujii, T. & Furukawa, Y. Identification of two Wnt-responsive elements in the intron of RING finger protein 43 (RNF43) Gene. *PLoS One* **9**, e86582 (2014).
13. Sandelin, A., Alkema, W., Engström, P., Wasserman, W. W. & Lenhard, B. JASPAR: an open-access database for eukaryotic transcription factor binding profiles. *Nucleic Acids Res.* **32**, (2004).
14. Thaler, R., Rumpler, M., Spitzer, S., Klaushofer, K. & Varga, F. Mospd1, a new player in mesenchymal versus epidermal cell differentiation. *J. Cell. Physiol.* **226**, 2505–2515 (2011).

15. Klass, M. R. & Hirsh, D. Sperm isolation and biochemical analysis of the major sperm protein from Caenorhabditis elegans. *Dev. Biol.* **84**, 299–312 (1981).
16. Sepsenwol, S., Ris, H. & Roberts, T. M. A unique cytoskeleton associated with crawling in the amoeboid sperm of the nematode, Ascaris suum. *J. Cell Biol.* **108**, 55–66 (1989).
17. Nelson, G. A., Roberts, T. M. & Ward, S. Caenorhabditis elegans spermatozoan locomotion : Amoeboid movement with almost no actin. *J. Cell Biol.* **92**, 121–131 (1982).
18. Kara, M. *et al.* A Role for MOSPD1 in mesenchymal stem cell proliferation and differentiation. *Stem Cells* **33**, 3077–3086 (2015).
19. Dancer, J. Y. *et al.* Expression of master regulatory genes controlling skeletal development in benign cartilage and bone forming tumors. *Hum. Pathol.* **41**, 1788–1793 (2010).
20. Confavreux, C. B. *et al.* Osteoid osteoma is an osteocalcinoma affecting glucose metabolism. *Osteoporos. Int. 2011 235* **23**, 1645–1650 (2011).
21. Groen, E. J. *et al.* Extra-intestinal manifestations of familial adenomatous polyposis. doi:10.1245/s10434-008-9981-3
22. León-Mateos, L. *et al.* Global gene expression characterization of circulating tumor cells in metastasic castration-resistant prostate cancer Patients. *J. Clin. Med* **2020**, 2066 (2066).
23. De La Taille, A. *et al.* β-catenin-related anomalies in apoptosis-resistant and hormone-refractory prostate cancer cells 1. (2003).
24. Puiffe, M.-L. *et al.* Characterization of ovarian cancer ascites on cell invasion, proliferation, spheroid formation, and gene expression in an in vitro model of epithelial ovarian cancer. *Neoplasia* **9**, 820–9 (2007).
25. Miwa, N. *et al.* Involvement of claudin-1 in the β-catenin/Tcf signaling pathway and its frequent upregulation in human colorectal cancers. *Oncol. Res.* **12**, 469–476 (2000).
26. Takahashi, M., Tsunoda, T., Seiki, M., Nakamura, Y. & Furukawa, Y. Identification of membrane-type matrix metalloproteinase-1 as a target of the β-catenin/Tcf4 complex in human colorectal cancers. *Oncogene* **21**, 5861–5867 (2002).
27. Takahashi, M., Nakamura, Y., Obama, K. & Furukawa, Y. Identification of SP5 as a downstream gene of the β-catenin/Tcf pathway and its enhanced expression in human colon cancer. *Int. J. Oncol.* **27**, 1483–1487 (2005).

28. Jho, E.-H. *et al.* Wnt/β-catenin/Tcf signaling induces the transcription of Axin2, a negative regulator of the signaling pathway. *Mol. Cell. Biol.* **22**, 1172–1183 (2002).
29. Yochum, G. S., Cleland, R. & Goodman, R. H. A genome-wide screen for β-catenin binding sites identifies a downstream enhancer element that controls c-Myc gene expression . *Mol. Cell. Biol.* **28**, 7368–7379 (2008).
30. Yamaguchi, K. *et al.* Overexpression of cohesion establishment factor DSCC1 through E2F in colorectal cancer. *PLoS One* **9**, (2014).

Acknowledgements

We thank Seira Hatakeyama and Yumiko Isobe (The University of Tokyo) for their technical assistance. This work was supported in part by the Grant-in-Aid #20K07563 (K.Y.) from the Japan Society for the Promotion of Science.

Author information

Author contributions

The experiments were designed by K.Y., and Y.F. The experiments were performed by C.H., C.Z., S.N., and Y.T. Data analysis was performed by C.H., C.Z., K.T., T.I., Y.O., S.A., G.T., Y.A., and D.S. The manuscript was written by C.H., K.Y., and Y.F. All authors critically read and approved the final paper.

Additional information

Conflict of interest

The authors declare no competing interests.

Figure Legends

Figure 1. MOSPD1 is regulated by the Wnt/β-catenin signaling in colorectal cancer. (a) Suppressed expression of MOSPD1 by β-catenin siRNAs in SW480 and HCT116 cells. (b) Induction of β-catenin in HeLa cells treated with LiCl (30 mM and 100 mM) increased MOSPD1 expression. The expression of β-actin served as a loading control. (c) Expression of *MOSPD1* in 104 CRC tissues and 25 non-tumorous colonic tissues. The data were obtained from a dataset of GSE21510 in GEO. Statistical significance was determined by unpaired t-test with Benjamini–Hochberg correction. (d) Scatter plots show the positive correlation between the expression levels of three Wnt target genes (*Y*-axis) and *MOSPD1* (*X*-axis). The data were obtained from GSE21510. (e) Immunohistochemical staining of β-catenin (upper) and MOSPD1 (lower) in CRC tissues. Scale bars 100 μm. Full-length, uncropped images are included within Supplementary Figure.

Figure 2. TCF7L2-interacting region in the 3'-flanking region may play a role as an enhancer. (a) Schematic representation of the ENCODE ChIP-seq data of TCF7L2, H3K4me1, and H3K27ac in HCT116 cells. (b) Reporter activity of

putative enhancer regions in the 5'- and 3'-flanking regions. HCT116 cells were transfected with pGL4.23 (Empty), pGL4.23-MOSPD1-5'E (MOSPD1-5'E), or pGL4.23-MOSPD1-3'E (MOSPD1-3'E) plasmids, in combination with pRL-null reporter plasmids for the normalization of transfection. The cells were co-transfected with pCAGGS-dnTCF7L2 plasmids expressing a dominant-negative form of TCF7L2 or the empty plasmids (Mock). Relative luciferase activities represent mean ± SD from three independent cultures. Statistical significance was determined by Student's t-test or Dunnett's test. (c) Effect of β-catenin siRNA on the reporter activity of pGL4.23-MOSPD1-3'E (MOSPD1-3'E) in HCT116 cells. Relative luciferase activities represent mean ± SD from three independent cultures. Statistical significance was determined by Dunnett's test. (d) ChIP-qPCR was performed using region-specific primer sets and the precipitants with an anti-TCF7L2 antibody or those with normal IgG. The amplification of a region upstream of *GAPDH* was used for normalization. The enhancer region in intron 2 of *RNF43* was used as a positive control. Data represents mean ± SD from three independent experiments. A significant difference was determined by Student's t-test.

Figure 3. Involvement of the three TBEs in the reporter activity. (a) Schematic representation of wild type (open circle: WWCAAAG, W: A/T) and mutant (closed circle: WWCAGCG) TCF-binding motifs in pGL4.23-MOSPD1-3'E reporter plasmids. (b) Relative reporter activity of empty, wild type and mutant reporter plasmids in HCT116 cells (WT, TBE1-mut, TBE2-mut, TBE3-mut, or TBEall-mut). The data represent mean ± SD from three independent cultures. Statistical significance was determined by Student's t-test or Dunnett's test.

Figure 1

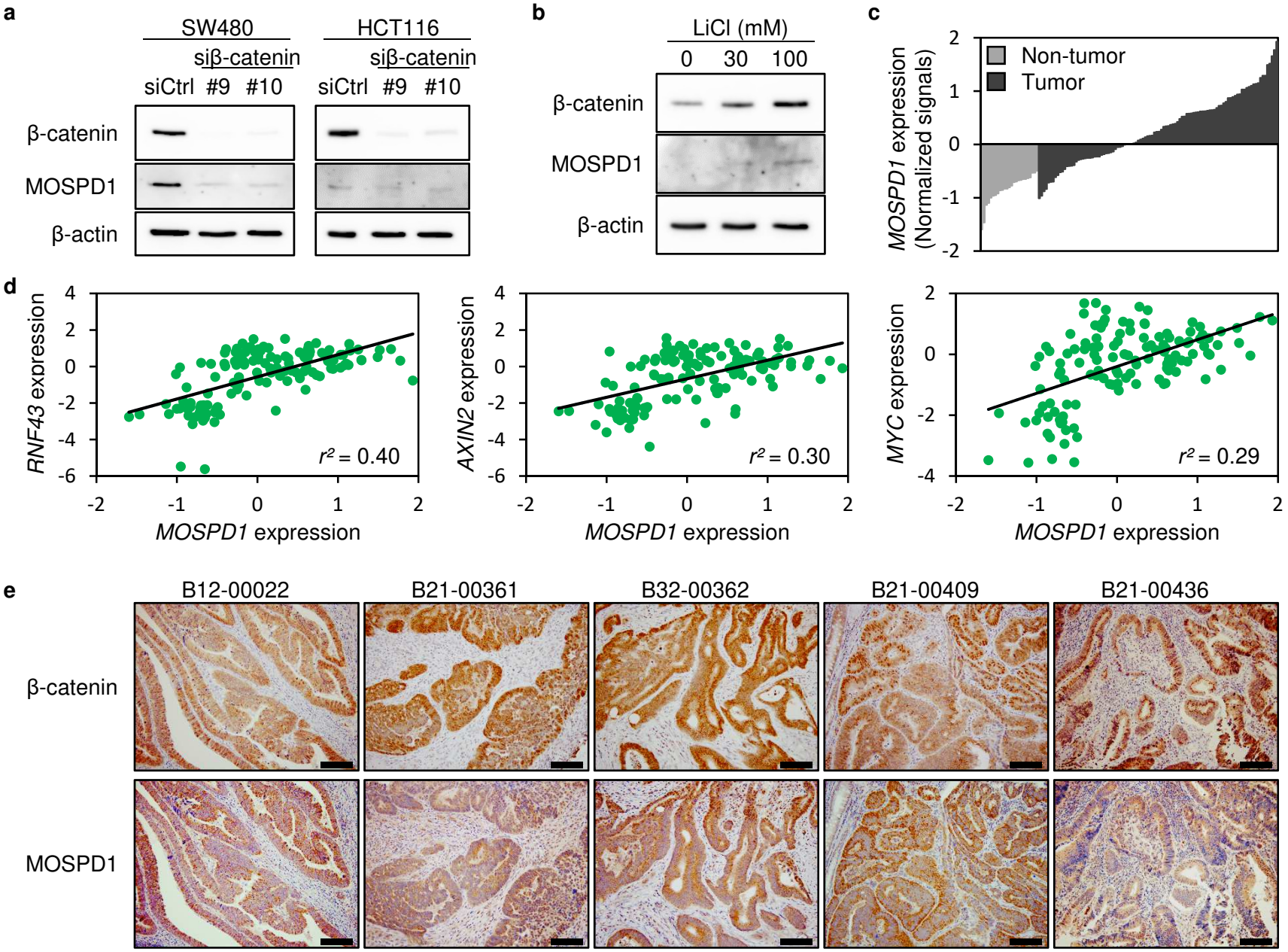
a
SW480
HCT116
siβ-catenin
siCtrl #9 #10
β-catenin
MOSPD1
β-actin
b
LiCl (mM)
0 30 100
β-catenin
MOSPD1
β-actin
c
MOSPD1 expression (Normalized signals)
Non-tumor
Tumor
d
RNF43 expression
AXIN2 expression
MYC expression
MOSPD1 expression
r² = 0.40
r² = 0.30
r² = 0.29
e
B12-00022
B21-00361
B32-00362
B21-00409
B21-00436
β-catenin
MOSPD1

Figure 2

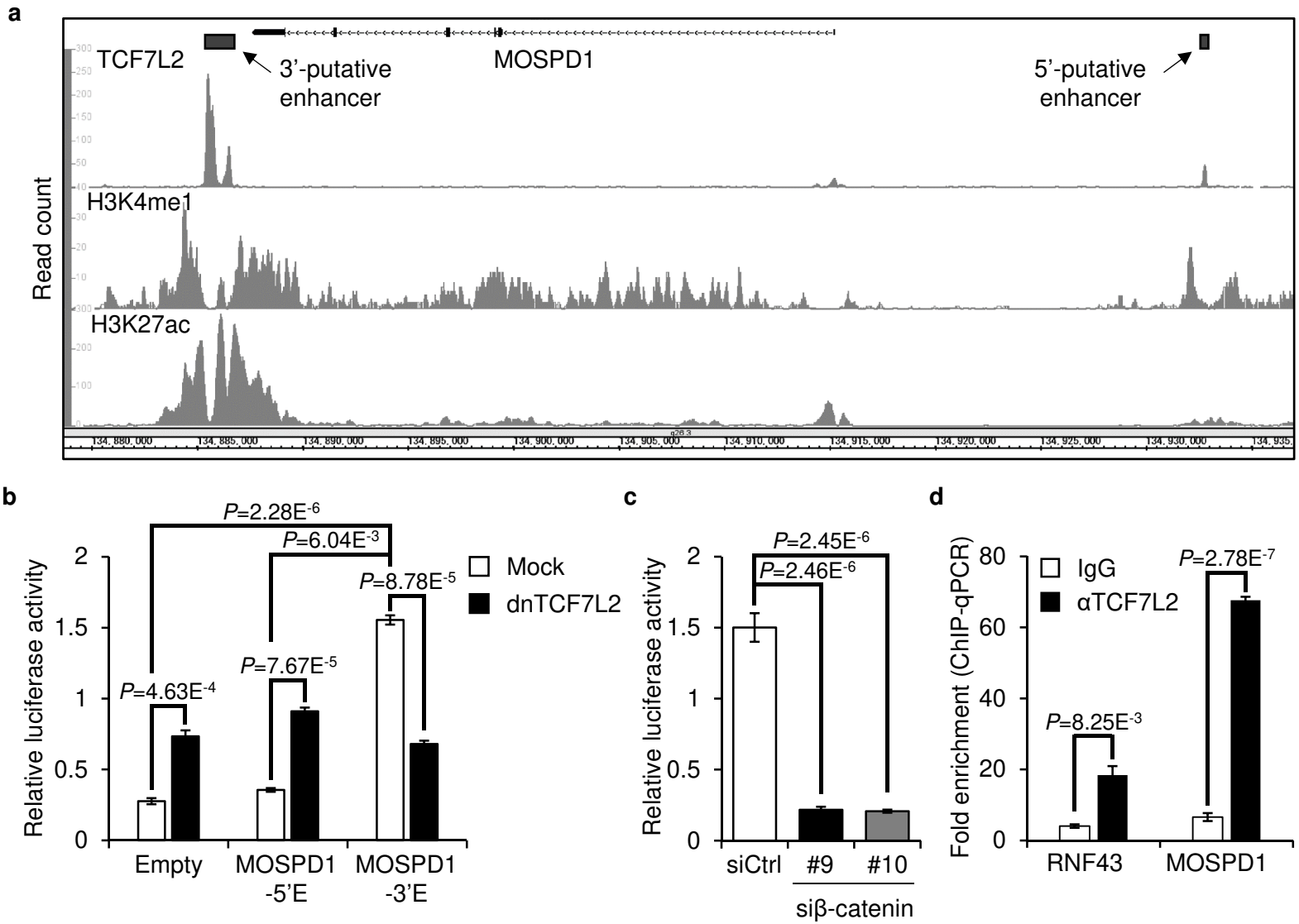
a
TCF7L2
3'-putative enhancer
MOSPD1
5'-putative enhancer
Read count
H3K4me1
H3K27ac
b
P=2.28E-6
P=6.04E-3
P=8.78E-5
P=4.63E-4
P=7.67E-5
Relative luciferase activity
Mock
dnTCF7L2
Empty
MOSPD1 -5'E
MOSPD1 -3'E
c
P=2.45E-6
P=2.46E-6
Relative luciferase activity
siCtrl
#9
#10
siβ-catenin
d
IgG
αTCF7L2
P=2.78E-7
P=8.25E-3
Fold enrichment (ChIP-qPCR)
RNF43
MOSPD1

Figure 3

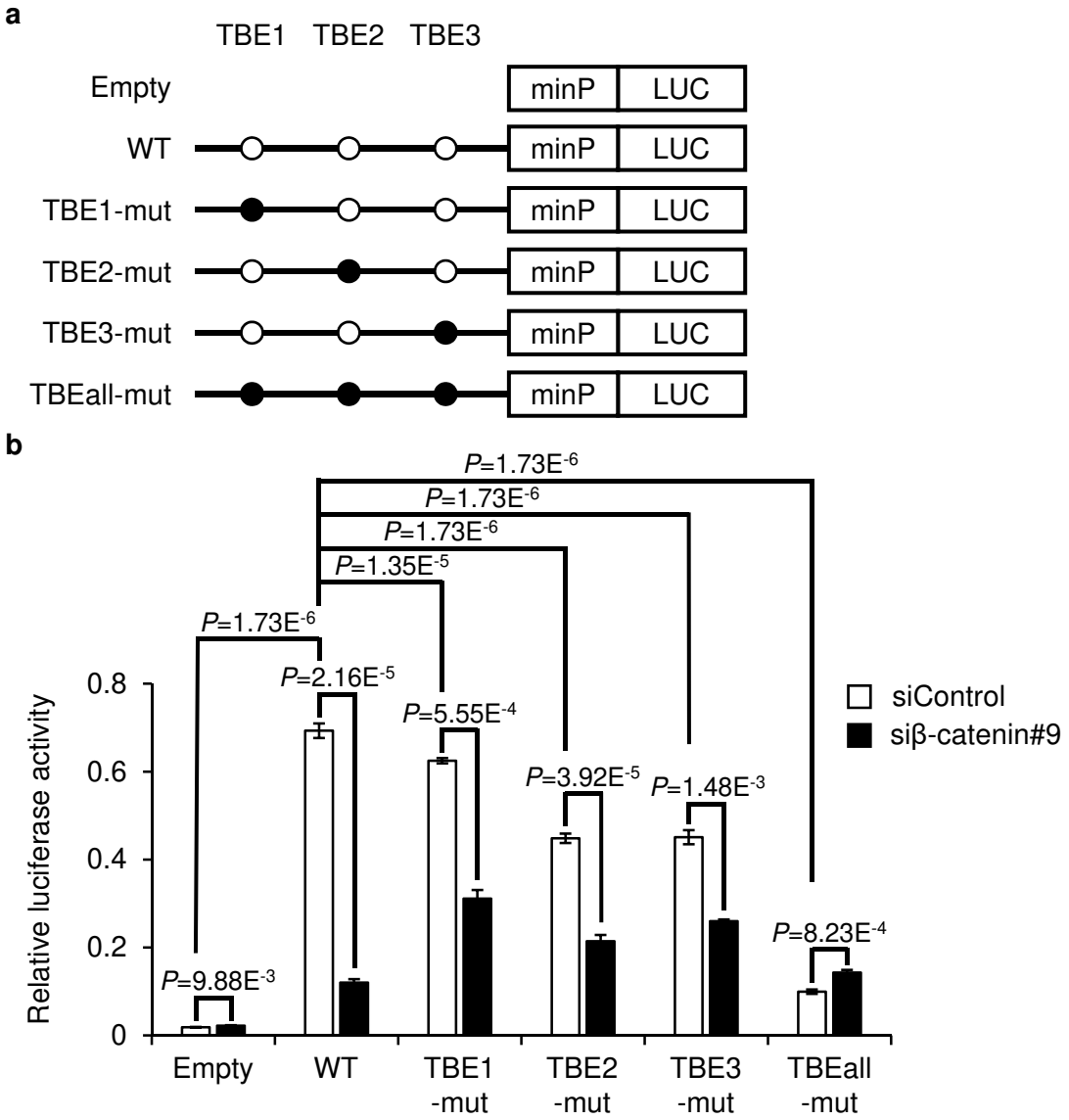
a
TBE1
TBE2
TBE3
Empty
WT
TBE1-mut
TBE2-mut
TBE3-mut
TBEall-mut
minP
LUC
b
P=1.73E-6
P=1.73E-6
P=1.73E-6
P=1.35E-5
P=1.73E-6
P=2.16E-5
P=5.55E-4
P=3.92E-5
P=1.48E-3
P=8.23E-4
P=9.88E-3
Relative luciferase activity
0.8
0.6
0.4
0.2
0
siControl
siβ-catenin#9
Empty
WT
TBE1 -mut
TBE2 -mut
TBE3 -mut
TBEall -mut

Supplementary Files

This is a list of supplementary files associated with this preprint. Click to download.

- Supplementarymaterials.pdf